

# The Correlation Between Wear and Lubricating Film Thickness in the Tribocorrosion of CoCrMo Alloy

Jinyu Li\*, Shoufan Cao and Zhanpeng Yang

School of Mechanical Engineering, Nanjing University of Science and Technology, 210094 Nanjing, China

**Abstract:** Tribocorrosion modelling of passive metals considering the lubrication effect from solution is still not well studied. A lubricated tribocorrosion model for CoCrMo alloy metal-on-metal hip joints has been developed, while the generalization of this model is restricted by Dowson's empirical correlation. This study explored the correlation between wear of CoCrMo alloy in tribocorrosion and lubricating film thickness. The results showed that the chemical, mechanical and total wear volumes of CoCrMo alloy in tribocorrosion were significantly influenced by the lubrication effect from the solution. Good correlations were obtained between the lubricating film thickness and chemical, mechanical and total wear, respectively. The new chemical and mechanical wear correlations could be used to generalize the current lubricated tribocorrosion model for CoCrMo alloy.

**Keywords :** CoCrMo alloy, Tribocorrosion, Lubrication, Model, Film thickness.

## 1. INTRODUCTION

The total material loss of passive metals in tribocorrosion was found not to be simply the sum of wear in absence of corrosion and the corrosion without wear [1-6]. The interaction between mechanical wear and electrochemical corrosion significantly accelerates material deterioration of passive metals. With better understanding of tribocorrosion mechanisms of passive metals, great progress in tribocorrosion modelling of passive metals has been observed in the last decades [7-11]. It should be noted that the solution surrounding the passive metals not only acts as a corrosive medium, causing corrosion of the metals, but also serves as lubricant, alleviating wear of the metals. However, tribocorrosion modelling taking into account the lubrication effect from the solution is still not well studied.

Based on the plastic deformation of contacting asperities in tribocorrosion of passive metals, Cao *et al.* [12] developed a lubricated tribocorrosion model that integrated the effect of chemical wear, mechanical wear and fluid lubrication on the total degradation of passive metals. By integrating an empirical correlation between the running-in wear of metal-on-metal (MoM) hip joints obtained from hip joint simulators and the minimum elastohydrodynamic film thickness, the model was applied to CoCrMo alloys. The results showed that the model accurately predicted the running-in wear of CoCrMo alloys observed in hip joint simulators [13]. The model was also used to rationalize the *in-vivo* degradation of MoM hip joints and the relevance of patient specific parameters on the wear and corrosion of MoM hip joints was highlighted.

Considering the successful application of this model in predicting the tribocorrosion of CoCrMo alloys used in MoM hip joints, the generalization of this model to other applications is of great importance. Cao's lubricated tribocorrosion model incorporated the Archard mechanical wear model and Mischler's wear accelerated corrosion model, which are both mechanistic approaches that are not restricted to MoM hip joints or CoCrMo alloys. However, the Dowson's running-in wear – minimum elastohydrodynamic film thickness empirical correlation (Equation (1)) [14] was extracted from CoCrMo alloys MoM hip joints, thus restricted the applicability of Cao's lubricated tribocorrosion model.

$$V_{\text{running-in}} (\text{mm}^3) = \frac{93.97}{(h_{\text{min}} (\text{nm}))^{1.49}} \quad (1)$$

Therefore, this study was initiated with the aim to explore the correlation between CoCrMo alloy's wear (chemical, mechanical and total) in tribocorrosion and the lubricating film thickness using experimental results obtained from universal laboratory tribometers. The modified correlations were expected to be incorporated into Cao's model in order to predict CoCrMo alloy's tribocorrosion in applications other than MoM hip joints.

## 2. TRIBOCORROSION EXPERIMENTAL DATA OF COCRMO ALLOYS

Guadalupe *et al.* [15] studied the tribocorrosion behavior of a high carbon CoCrMo alloy in 0.5 M sulphuric acid ( $\text{H}_2\text{SO}_4$ ) using a reciprocating motion tribometer incorporated with a three-electrode electrochemical cell. The experimental setup is schematically shown in Figure 1. An alumina ball was sliding on the CoCrMo alloy disk. The CoCrMo alloy sample acted as working electrode, a platinum wire coil as counter electrode, and a mercuric sulfate electrode

\*Address correspondence to this author at the School of Mechanical Engineering, Nanjing University of Science and Technology, 210094 Nanjing, China;  
E-mail: jinyu.li@njust.edu.cn

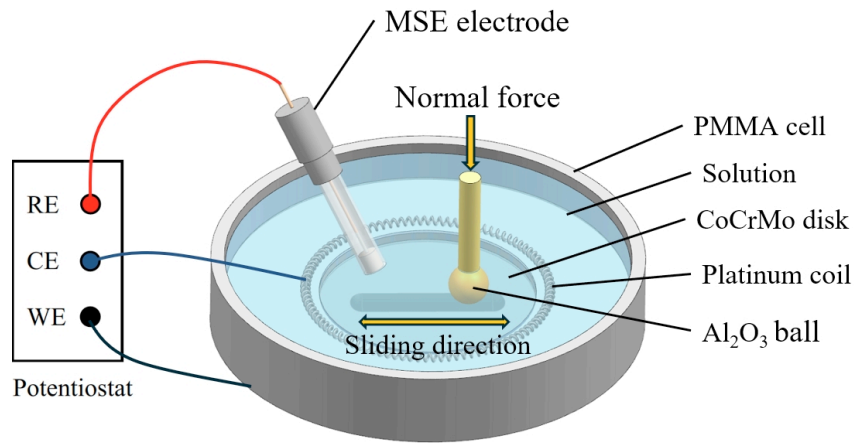


**Figure 1:** Tribocorrosion setup including a reciprocating tribometer and a three-electrode electrochemical cell.

(MSE) as reference electrode. The tribocorrosion experiments were conducted under different normal forces. Cao *et al.* [16] further studied the effect of solution viscosity on tribocorrosion of CoCrMo alloy by mixing 0.5 M H<sub>2</sub>SO<sub>4</sub> solution with glycerol in order to modify the solution viscosity. The same CoCrMo alloy as used in [15] was adopted and the experiments were conducted using the same tribocorrosion setup as that in [15]. In this study, we extracted the friction and wear results from [15, 16], and further studied the correlation between the theoretical elastohydrodynamic film thickness and chemical, mechanical and total wear, respectively.

### 2.1. Values of the Experimental Parameters

The values of the extracted experimental parameters from [15, 16] are summarized in Table 1. A dwell time of 0.25 s was set after each stroke, which results in a sliding velocity of 20 mm/s considering a stroke length of 5 mm and a reciprocating frequency of 1 Hz. It should be noted that the tribometer used in [15] and [16] adopted a powerful motor with high accelerating rate (10 m/s<sup>2</sup>) to ensure a constant sliding velocity during sliding.

### 2.2. Friction Coefficient and Wear Volumes

Table 2 summarizes the average coefficient of friction (CoF) as well as total, chemical and mechanical wear volumes of CoCrMo alloy disks extracted from [15] and [16]. The average CoF was calculated by averaging the instant friction coefficient during sliding. Total wear volume  $V_{tot}$  was calculated by multiplying the area of each wear track's cross-sectional profile by the length of the wear track. Chemical wear volume  $V_{chem}$  was calculated from the measured anodic current during sliding by applying the Faraday's law, as shown in Equation (2):

$$V_{chem} = \frac{I_r \cdot t \cdot M}{n \cdot F \cdot \rho} \quad (2)$$

where,  $I_r$  is anodic current,  $t$  is sliding time,  $M$  is molecular mass of the CoCrMo alloy (58.66 g/mol),  $n$  is charge number of the alloy (2.37),  $F$  is Faraday's constant (approximately 96,500 C/mol),  $\rho$  is density of the alloy (8.33 g/cm<sup>3</sup>).

**Table 1: Values of the Experimental Parameters**

Parameter	Value in Guadalupe <i>et al.</i> [15]	Value in Cao <i>et al.</i> [16]
Al <sub>2</sub> O <sub>3</sub> ball diameter	6 mm	6 mm
Normal force	5.8 N, 11.7 N, 17.5 N	5.6 N
Applied potential	0 V <sub>MSE</sub>	0 V <sub>MSE</sub>
Stroke length	5 mm	5 mm
Reciprocating frequency	1 Hz	1 Hz
Total testing time	1800 s	1800 s
Solution	0.5 M H <sub>2</sub> SO <sub>4</sub>	100 % 0.5 M H <sub>2</sub> SO <sub>4</sub> +0 % Glycerol, 60 % 0.5 M H <sub>2</sub> SO <sub>4</sub> +40 % Glycerol, 40 % 0.5 M H <sub>2</sub> SO <sub>4</sub> +60 % Glycerol, 20 % 0.5 M H <sub>2</sub> SO <sub>4</sub> +80 % Glycerol, 5 % 0.5 M H <sub>2</sub> SO <sub>4</sub> +95 % Glycerol

Table 2: Summary of the Results Obtained from the Tribocorrosion Tests

Glycerol content [vol.%]	Normal force [N]	CoF	Total wear [ $10^{-3}$ mm <sup>3</sup> ]	Chemical wear [ $10^{-3}$ mm <sup>3</sup> ]	Mechanical wear [ $10^{-3}$ mm <sup>3</sup> ]	Lubricating film thickness [nm]
0	5.6	0.26 ± 0.01	4.67 ± 0.24	3.32	1.35	0.12
		0.30 ± 0.02	4.72 ± 0.15	3.32	1.40	
	5.8	0.27 ± 0.01	6.56 ± 0.12	3.95	2.61	0.12
		0.28 ± 0.01	6.67 ± 1.78	4.00	2.67	
	11.7	0.25 ± 0.01	10.16 ± 0.36	6.10	3.13	0.11
		0.26 ± 0.01	9.80 ± 0.28	6.47	3.33	
17.5	0.25 ± 0.01	15.61 ± 0.99	8.60	7.01	0.10	
	0.28 ± 0.02	17.69 ± 1.58	8.31	9.38		
40	5.6	0.29 ± 0.02	2.45 ± 0.05	1.61	0.84	0.31
		0.27 ± 0.02	2.64 ± 0.05	1.71	0.93	
60	5.6	0.25 ± 0.01	1.10 ± 0.06	0.8	0.30	0.63
		0.24 ± 0.02	1.01 ± 0.07	0.74	0.27	
80	5.6	0.16 ± 0.03	0.43 ± 0.03	0.31	0.12	1.90
		0.15 ± 0.02	0.48 ± 0.07	0.37	0.11	
95	5.6	0.09 ± 0.01	0.05 ± 0.02	0.04	0.01	6.31
		0.11 ± 0.02	0.08 ± 0.01	0.06	0.02	

The mechanical wear volume  $V_{mech}$  was determined by subtracting the total wear volume by the chemical wear volume, as shown in Equation (3):

$$V_{mech} = V_{tot} - V_{chem} \quad (3)$$

### 2.3. The Minimum Lubricating Film Thickness Calculation

The theoretical minimum elastohydrodynamic film thickness for the above experiments was calculated using the Hamrock-Dowson equation [17]:

$$h_{min} = 2.8 \left( \frac{u\eta}{E'R'} \right)^{0.65} \left( \frac{F_n}{E'R'^2} \right)^{-0.21} R' \quad (4)$$

In this equation,  $u$  is entraining velocity,  $u = (v_{s1} + v_{s2})/2$ .  $v_{s1}$  and  $v_{s2}$  are velocities of the two counterparts. Since  $v_{s1} = 20$  mm/s and  $v_{s2} = 0$ ,  $u = 10$  mm/s.  $\eta$  is the viscosity of the solution. The viscosities of the H<sub>2</sub>SO<sub>4</sub>-glycerol mixtures measured by Cao *et al.* [16] are listed in Table 3.

$E'$  is effective Young's modulus calculated using Equation (5):

$$\frac{2}{E'} = \left( \frac{1 - \nu_1^2}{E_1} + \frac{1 - \nu_2^2}{E_2} \right) \quad (5)$$

where,  $E_1$ ,  $\nu_1$  and  $E_2$ ,  $\nu_2$  are Young's modulus and Poisson's ratio of the CoCrMo alloy and Al<sub>2</sub>O<sub>3</sub>,

respectively. Since  $E_1 = 248$  GPa,  $\nu_1 = 0.3$  and  $E_2 = 350$  GPa,  $\nu_2 = 0.22$ , the resulted  $E'$  is 313.08 GPa.

Table 3: Viscosity of the H<sub>2</sub>SO<sub>4</sub>-Glycerol Mixtures

Solution		Viscosity
0.5 M H <sub>2</sub> SO <sub>4</sub>	Glycerol	[mPa·s]
100 vol.%	0 vol.%	1.2 ± 0.4
60 vol.%	40 vol.%	4.9 ± 0.6
40 vol.%	60 vol.%	14.8 ± 1.8
20 vol.%	80 vol.%	80.5 ± 6.4
5 vol.%	95 vol.%	511.4 ± 19.2

$R'$  is composite radius of curvature, which can be calculated using Equation (6):

$$\frac{1}{R'} = \frac{1}{R_1} + \frac{1}{R_2} \quad (6)$$

where,  $R_1$  and  $R_2$  are the radius of the two contacting bodies, respectively. Since  $R_1 = 3$  mm and  $R_2 = +\infty$ ,  $R' = 3$  mm.

Considering the different normal forces used in [15] and different solution viscosities adopted in [16], the theoretical minimum film thickness for each experimental condition was calculated and added into Table 2.

### 3. THE CORRELATION BETWEEN LUBRICATING FILM THICKNESS AND THE FRICTION AND WEAR OF COCRMO ALLOY IN TRIBOCORROSION

#### 3.1. Variation of CoF with the Increase of Lubricating Film Thickness

Figure 2 plots the measured CoF against the calculated minimum lubricating film thickness.

In general, the CoF showed a decreasing trend with the increase of lubricating film thickness. Based on the Stribeck curve [18], these experiments were mostly conducted in the mixed lubrication regime. In 0.5 M H<sub>2</sub>SO<sub>4</sub> solution without glycerol, the CoF was between 0.25 and 0.3 under all of the four normal forces and the CoF didn't show a clear reduction with the decrease of normal force. This can be explained by the very slight increase of lubricating film thickness from 5.6 N to 17.5 N that could not lead to a significant improvement of the lubrication condition. While with the increase of glycerol content, the lubrication was dramatically promoted, thus the CoF was decreased gradually. This indicates that the prevailing lubrication regime was mixed lubrication. The CoF was reduced to around 0.1 in the solution with 95 vol.% glycerol.

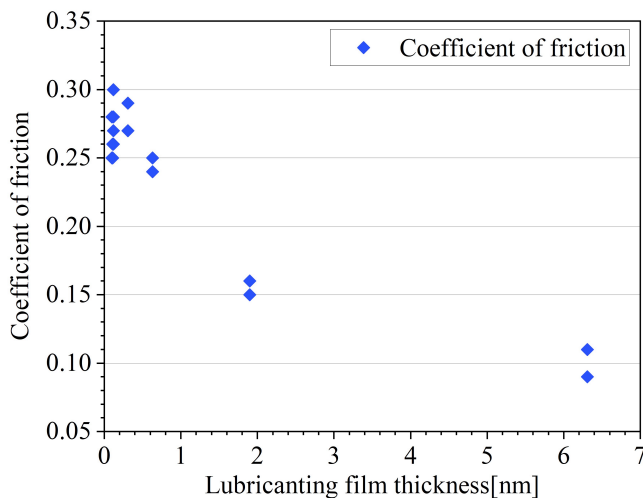


**Figure 2:** Variation of CoF with the increase of lubricating film thickness.

#### 3.2. Variation of Wear with the Increase of Lubricating Film Thickness

Figure 3 to Figure 5 depict the variation of chemical, mechanical and total wear volume with the increase of calculated minimum lubricating film thickness. All of the three types of wear volumes were found to decreasing when the lubricating film thickness was getting higher. This clearly shows that both electrochemical corrosion and mechanical wear of CoCrMo alloy in tribocorrosion were significantly influenced by the lubrication effect from the solution.

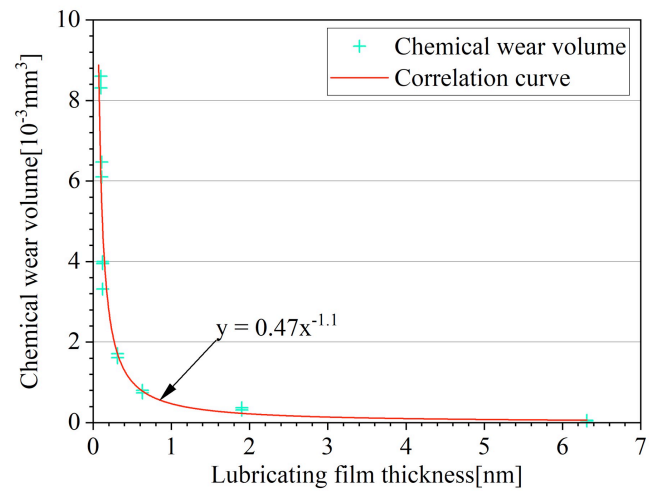


**Figure 3:** Variation of chemical wear volume with the increase of lubricating film thickness.

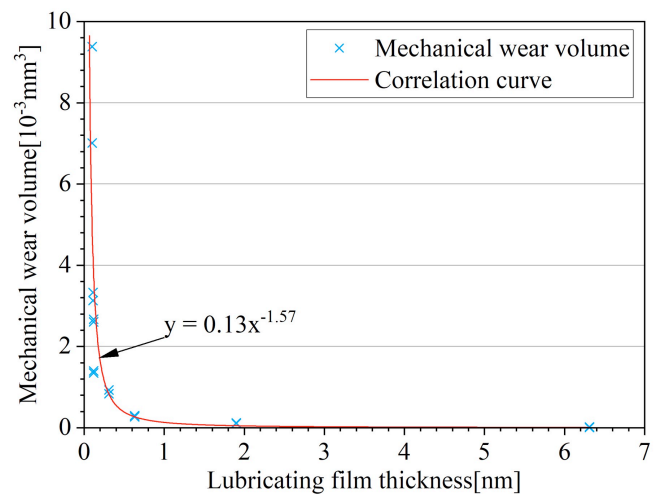


**Figure 4:** Variation of mechanical wear volume with the increase of lubricating film thickness.

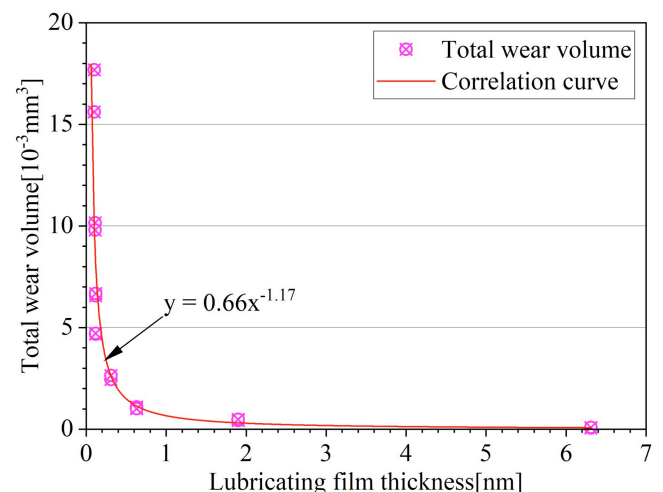


**Figure 5:** Variation of total wear volume with the increase of lubricating film thickness.

## 4. DISCUSSION

Dowson's empirical correlation between the running-in wear and minimum lubricating film thickness obtained from MoM hip joint simulator experiments

indicated a power function between the running-in wear and minimum lubricating film thickness, as shown in Equation (1). Thus, it was attempted to apply a power function to the chemical, mechanical and total wear in Figure 3 to Figure 5. The obtained correlation curves were added into the Figure 3 to Figure 5. Surprisingly, all of the chemical, mechanical and total wear volume showed good correlations with the lubricating film thickness under a power function. On the other hand, it could also be observed from Figure 3 to Figure 5 that even the power values for the chemical, mechanical and total wear were different, they are all between -1.1 and -1.6. Dowson's correlation only considered the total wear and it is interesting to see that the power values found in Figure 3 to Figure 5 are quite close to Dowson's value (-1.49) even they are obtained from relatively different testing machines and solutions.

Extracted from Figure 3 to Figure 5, Equations (7) to (9) summarized the correlations between theoretical minimum lubricating film thickness and the chemical, mechanical and total wear of CoCrMo alloy, respectively. Since the results in this study were obtained from experiments conducted using a universal tribometer, Equations (7) to (9) are more representative of the real relationship between lubricating film thickness and electrochemical corrosion as well as mechanical wear of CoCrMo alloy.

$$V_{chem} = 0.47h_{min}^{-1.1} \quad (7)$$

$$V_{mech} = 0.13h_{min}^{-1.57} \quad (8)$$

$$V_{tot} = 0.66h_{min}^{-1.17} \quad (9)$$

## 5. CONCLUSION

In this study, the correlation between wear of CoCrMo alloy and theoretical lubricating film thickness in tribocorrosion was explored and the following conclusions are drawn:

1. With the increase of lubricating film thickness, the coefficient of friction in the tribocorrosion experiments showed a clearly decreasing trend, which indicated that the prevailing lubrication regime was mixed lubrication.
2. The chemical, mechanical and total wear volumes of CoCrMo alloy all showed dramatical decrease with the increase of lubricating film thickness, which demonstrated the importance of lubrication on the tribocorrosion property of CoCrMo alloy.
3. Good correlations were obtained between the lubricating film thickness and chemical, mechanical and total wear of CoCrMo alloy,

respectively. Moreover, the new correlations were found to be close to Dowson's correlation. The new chemical and mechanical wear correlations could be used to generalize Cao's lubricated tribocorrosion model for CoCrMo alloy.

## ACKNOWLEDGEMENT

This research was funded by the Fundamental Research Funds for the Central Universities, China (No. 30923010932, No. 309231B8802) and the Jiangsu Provincial Double – Innovation Doctor Program (No. JSSCBS20220251).

## CONFLICTS OF INTEREST

The authors declared no conflict of interest.

## REFERENCES

- [1] Yan C, Zhang Y, Zeng Q, *et al.* Comparative Investigation on the Tribocorrosion Resistance of Ti6Al4V and 60NiTi Alloys in Simulated Seawater Environment [J]. *Wear*, 2024: 205423. <https://doi.org/10.1016/j.wear.2024.205423>
- [2] Zhou Y, Zhao Z, Jiang S, *et al.* Effect of heat treatment on the tribocorrosion behavior of 20Cr13 martensitic stainless steel [J]. *Tribology International*, 2024; 197: 109768. <https://doi.org/10.1016/j.triboint.2024.109768>
- [3] Chen H, Li R P, Liu L Y, *et al.* Structural, mechanical and tribocorrosion behaviors of Mo-Ni-Si alloys [J]. *Tribology International*, 2024; 196: 109723. <https://doi.org/10.1016/j.triboint.2024.109723>
- [4] Yilmazer H, Caha I, Dikici B, *et al.* Investigation of the influence of high-pressure torsion and solution treatment on corrosion and tribocorrosion behavior of cocrmo alloys for biomedical applications [J]. *Crystals*, 2023; 13(4): 590. <https://doi.org/10.3390/cryst13040590>
- [5] Stemp M, Mischler S, Landolt D. The effect of mechanical and electrochemical parameters on the tribocorrosion rate of stainless steel in sulphuric acid [J]. *Wear*, 2003; 255(1-6): 466-475. [https://doi.org/10.1016/S0043-1648\(03\)00085-1](https://doi.org/10.1016/S0043-1648(03)00085-1)
- [6] Stojadinović J, Bouvet D, Declercq M, *et al.* Effect of electrode potential on the tribocorrosion of tungsten [J]. *Tribology International*, 2009, 42(4): 575-583. <https://doi.org/10.1016/j.triboint.2008.04.009>
- [7] Landolt D, Mischler S, Stemp M. Electrochemical methods in tribocorrosion: a critical appraisal [J]. *Electrochimica acta*, 2001; 46(24-25): 3913-3929. [https://doi.org/10.1016/S0013-4686\(01\)00679-X](https://doi.org/10.1016/S0013-4686(01)00679-X)
- [8] López-Ortega A, Arana J L, Bayón R. Tribocorrosion of passive materials: a review on test procedures and standards [J]. *International Journal of Corrosion*, 2018; 2018(1): 7345346. <https://doi.org/10.1155/2018/7345346>
- [9] Jemmely P, Mischler S, Landolt D. Electrochemical modeling of passivation phenomena in tribocorrosion [J]. *Wear*, 2000, 237(1): 63-76. [https://doi.org/10.1016/S0043-1648\(99\)00314-2](https://doi.org/10.1016/S0043-1648(99)00314-2)
- [10] Mischler S, Debaud S, Landolt D. Wear accelerated corrosion of passive metals in tribocorrosion systems [J]. *Journal of the Electrochemical society*, 1998; 145(3): 750. <https://doi.org/10.1149/1.1838341>
- [11] Mischler S. Triboelectrochemical techniques and interpretation methods in tribocorrosion: A comparative evaluation [J]. *Tribology International*, 2008; 41(7): 573-583. <https://doi.org/10.1016/j.triboint.2007.11.003>

- [12] Cao S, Maldonado S G, Mischler S. Tribocorrosion of passive metals in the mixed lubrication regime: theoretical model and application to metal-on-metal artificial hip joints [J]. *Wear*, 2015; 324: 55-63. <https://doi.org/10.1016/j.wear.2014.12.003>
- [13] Cao S, Mischler S. Assessment of a recent tribocorrosion model for wear of metal-on-metal hip joints: Comparison between model predictions and simulator results [J]. *Wear*, 2016, 362: 170-178. <https://doi.org/10.1016/j.wear.2016.05.025>
- [14] Dowson, D. Tribological principles in metal-on-metal hip joint design [J]. *Proceedings of the Institution of Mechanical Engineers, Part H: Journal of Engineering in Medicine*, 2006, 220:161-171. <https://doi.org/10.1243/095441105X63255>
- [15] Guadalupe Maldonado S, Mischler S, Cantoni M, *et al.* Mechanical and chemical mechanisms in the tribocorrosion of a Stellite type alloy [J]. *Wear*, 2013; 308(1-2): 213-221. <https://doi.org/10.1016/j.wear.2013.04.007>
- [16] Cao S, Mischler S. Tribocorrosion of a CoCrMo alloy in sulfuric acid–glycerol mixtures [J]. *Wear*, 2020; 458: 203443. <https://doi.org/10.1016/j.wear.2020.203443>
- [17] Hamrock B J, Dowson D. Elastohydrodynamic lubrication of elliptical contacts for materials of low elastic modulus I—fully flooded conjunction [J]. *Lubrication Tech*, 1978; 100(2): 236-245. <https://doi.org/10.1115/1.3453152>
- [18] Kalin M, Velkavrh I, Vižintin J. The Stribeck curve and lubrication design for non-fully wetted surfaces [J]. *Wear*, 2009; 267(5-8): 1232-1240. <https://doi.org/10.1016/j.wear.2008.12.072>

---

Received on 08-11-2024

Accepted on 12-12-2024

Published on 17-12-2024

<https://doi.org/10.31875/2409-9848.2024.11.07>

© 2024 Li *et al.*

This is an open-access article licensed under the terms of the Creative Commons Attribution License (<http://creativecommons.org/licenses/by/4.0/>), which permits unrestricted use, distribution, and reproduction in any medium, provided the work is properly cited.